Letter to the Editor

Syntelin inhibits triple-negative breast cancer cell proliferation and metastasis

Dear Editor,

The hallmarks of cancer comprise several distinct biological characteristics acquired during the multistep development of human tumors with the unique feature of genomic instability (Shen, 2011). These cancer characteristics include sustaining proliferative signaling, evading growth suppressors, resisting cell death, enabling replicative immortality, inducing angiogenesis, and activating invasion and metastasis (Chen et al., 2011; Song et al., 2018). Triple-negative breast cancer (TNBC), an aggressive disease with increased risks for visceral metastases, has a poor prognosis due to unavailable and viable therapeutic targets (Bianchini et al., 2016). A TNBC diagnosis indicates that cancer cells test negative for three key receptors: estrogen receptor, progesterone receptor, and human epidermal growth factor receptor 2 (Bianchini et al., 2016). The absence of these three receptors renders existing hormone and targeted therapies ineffective.

Kinesin proteins serve as potential targets for cancer therapy due to their aberrant overexpression, association with malignancy, and drug resistance in solid tumors (Rath and Kozielski, 2012). Centromere-associated protein E (CENP-E), a mitotic kinesin, is an essential protein that regulates metaphase chromosome alignment and central spindle assembly (Huang et al., 2019; Liu et al., 2020). Recent genomic analyses suggest the

function of CENP-E in TNBC progression (Kung et al., 2014), which prompted us to evaluate the efficacy of the CENP-E chemical inhibitor syntelin (Figure 1A) in TNBC chemotherapy. Syntelin is a first-in-class chemical inhibitor of CENP-E that blocks the release of ADP and locks CENP-E–microtubule interaction (Ding et al., 2010), which results in syntelic attachment of sister kinetochores steadily linked to microtubules and subsequent mitotic arrest (Liu et al., 2020).

Here, we report the chemotherapeutic efficacy of syntelin in TNBC. Our preliminary screen of CENP-E in various breast cancer cell lines indicated its high protein levels in TNBC cell lines, such as MDA-MB-231 cells (Supplementary Figure S1A), consistent with the aforementioned genetic analyses and TCGA database (Kung et al., 2014). To evaluate whether syntelin inhibits MDA-MB-231 cell proliferation, we carried out time-course analyses using an MTT assay that involves the conversion of the water-soluble yellow dye MTT to an insoluble purple formazan by the action of mitochondrial reductase. Formazan is then solubilized and the concentration is determined by optical density at 570 nm. As shown in Figure 1B, syntelin and taxol exhibited little effect on MDA-MB-231 cell growth at an initial interval of 0.5 h. However, a long-term treatment of 12–15 h resulted in a significant inhibition of cell proliferation compared to the control group ($P < 0.001$; Figure 1B and Table 1) without altering CENP-E protein level (Supplementary Figure S1B).

Previous studies have established the dynamic distribution pattern of CENP-E in HeLa cells (Yao et al., 1997). We next sought to test the subcellular distribution of CENP-E in MDA-MB-231 cells. As shown

in Supplementary Figure S2A, CENP-E is associated with kinetochore in control metaphase cells (top panel) and relocated to the central spindle and midbody (third panel), similar to what was observed in other cell types. However, the majority of syntelin-treated cells were arrested in the prometaphase with misaligned chromosomes, consistent with the role of CENP-E seen in HeLa cells. As a control, taxol stabilized the microtubule polymers and blocked cell division (Supplementary Figure S2A). Our statistical analyses show that syntelin treatment resulted in a significant increase in cells bearing misaligned chromosomes ($33\% \pm 4.2\%$; $P < 0.01$; Supplementary Figure S2B). To evaluate the precise impact of syntelin treatment on MDA-MB-231 cell division, real-time imaging analyses were carried out. As shown in Figure 1C, control cells progress through mitotic anaphase within 35 min, while syntelin-treated cells remain in metaphase after 70 min, indicating that syntelin blocks metaphase–anaphase transition.

Given the observed inhibition of MDA-MB-231 cell proliferation and division by syntelin, we sought to understand whether inhibition of CENP-E alters cell fate. Specifically, we probe whether syntelin alters necrosis vs. apoptosis using apopxin and 7-AAD as the reporter of apoptosis and necrosis, respectively. As shown in Figure 1D, syntelin-treated cells exhibited positive staining of apopxin without labeling of 7-AAD, while taxol treatment resulted in both increased apoptosis and necrosis judged by the intensities of apopxin and 7-AAD labeling, respectively. Our statistical analyses, from three independent experiments, show that taxol induced necrosis >5-fold
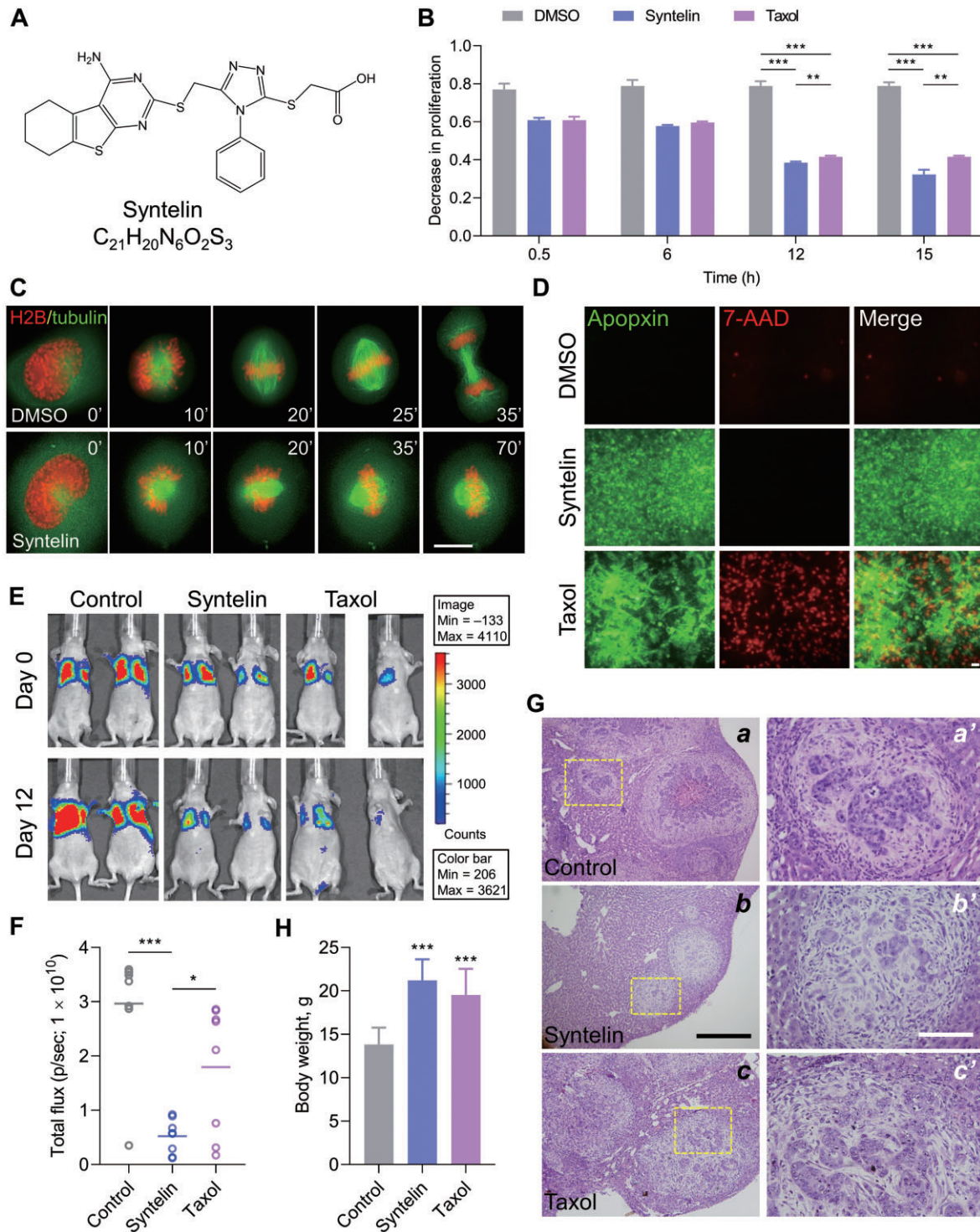
Figure 1 Syntelin inhibits cell proliferation and metastasis in TNBC. (**A**) Chemical structure of syntelin. (**B**) MDA-MB-231 cells were treated with either syntelin or taxol at 2 μM for various intervals using MTT assay to assess a time-dependent drug response. Data represent mean ± SEM from three independent experiments. **$P < 0.01$; ***$P < 0.001$. (**C**) Real-time imaging of MDA-MB-231 cell division indicates a mitotic blockage by syntelin. Scale bar, 10 μm. (**D**) MDA-MB-231 cells were stained with Apopxin (green) and 7-AAD (red) to visualize apoptosis and necrosis, respectively. Scale bar, 10 μm. (**E**) Representative images of tumor-bearing mice from mammary fat pad inoculation of MDA-MB-231 cells. (**F**) Quantification of bioluminescent signals (photons/sec) from mice inoculated with MDA-MB-231 cells. Data represent mean ± SD; $n = 8$. *$P < 0.05$; ***$P < 0.001$. (**G**) Representative H&E staining images of xenografts. Magnified images are also shown. Scale bar: left, 500 μm; right, 150 μm. (**H**) Body weight of tumor-bearing mice. Data represent mean ± SD; $n = 8$. ***$P < 0.001$ compared with control-treated mice.

Table 1 Comparison of the decrease in proliferation of the control, syntelin (2 μM), and taxol (2 μM) groups.

Time	Comparison groups	Absorbance	Adjusted *P*-value
12 h	Syntelin vs. Taxol	0.463 ± 0.037 vs. 0.437 ± 0.024	0.867
	Control vs. Syntelin	0.73 ± 0.043 vs. 0.463 ± 0.037	<0.001
	Control vs. Taxol	0.73 ± 0.043 vs. 0.437 ± 0.024	<0.001
15 h	Syntelin vs. Taxol	0.439 ± 0.042 vs. 0.422 ± 0.026	0.942
	Control vs. Syntelin	0.742 ± 0.041 vs. 0.439 ± 0.042	<0.001
	Control vs. Taxol	0.742 ± 0.041 vs. 0.422 ± 0.026	<0.001

MTT assay was used to determine proliferation in the control, syntelin, and taxol groups. Absorbance was measured with the spectrophotometer following the MTT assay. The *P*-values indicate that the differences between syntelin and taxol at 12 and 15 h were not statistically significant, thus implying that both drugs were equally effective at decreasing cell proliferation.

more than syntelin did ($P < 0.01$) but yielded nearly equal amounts of apoptotic and necrotic cells (Supplementary Figure S3A). Thus, syntelin is much more effective at inducing MDA-MB-231 cell apoptosis than necrosis compared to taxol.

Bcl-2 is an anti-apoptosis protein whose expression is indicative of uncontrolled proliferation, while Taxol-elicited Bcl-2 phosphorylation at Ser70 and cleaved caspase-3 induce apoptosis (Song et al., 2018). Our western blotting analysis demonstrated that taxol elevated the levels of phosphorylated Ser70-Bcl-2 and cleaved caspase-3 in MDA-MB-231 cells (Supplementary Figure S4). Interestingly, syntelin exhibited little effect on Bcl-2 phosphorylation and caspase-3 activation but dramatically increased the level of Bax, an apoptotic inducer (Supplementary Figure S4). Thus, syntelin inhibits MDA-MB-231 cell proliferation by promoting Bax-elicited apoptosis.

We next examined whether syntelin treatment interrogates TNBC progression in mice. To this end, we inoculated MDA-MB-231 cells into the mammary fat pads of NOD/SCID mice as reported (Chen et al., 2011). When the xenografts were palpable, the mice were given daily intraperitoneal injections of syntelin, taxol, or vehicle control. As shown in Figure 1E, the control xenografts exhibit growth and metastasis of MDA-MB-231 cells 12 days after inoculation. After 5 doses of syntelin treatment, tumor sizes were apparently shrunk judged by bioluminescent signals (photons/sec). The decreased trends of bioluminescent signals were also seen in taxol-treated mice after 12 days (Supplementary Figure S5A). Statistical analyses show that bioluminescent signals were significantly reduced by syntelin and taxol administration (Figure 1F). The careful examination also revealed that

liver metastasis was dramatically suppressed as evident by gross histological analysis (Supplementary Figure S5B). Hematoxylin–eosin (H&E) staining show massive metastasis in the livers from mice receiving vehicle control (Figure 1G; *a*, boxed; enlarged in *a'*), while syntelin treatment significantly decreased the number of metastatic nodules (Figure 1G, *b* and *b'*; Supplementary Figure S5C, $P < 0.001$ vs. Control, $n = 8$). In addition, syntelin reversed a reduction in mouse body weight (Figure 1H). As a positive control, taxol also inhibited liver metastasis of MDA-MB-231 cells. Thus, we conclude that syntelin minimizes TNBC metastasis.

Our findings uncover a novel action underlying CENP-E-targeted interrogation of TNBC progression. Thus, syntelin represents an emerging targeted chemotherapeutic intervention for the treatment of TNBC, which is worthy of further clinical investigation. The differential effects of syntelin on promoting apoptosis rather than necrosis exhibit surprising benefits for syntelin-based therapeutics. Our data indicate that chemotherapeutic drugs, such as taxol, currently among primary treatments for breast cancer, induces necrosis and inflammation. Given the fact that syntelin exhibits little detectable effect on the promotion of necrosis, it may represent an innovative cancer therapy that minimizes the impact of inflammation during chemotherapy.

In conclusion, this study has characterized the mechanism of action underlying syntelin-based interrogation of TNBC progression in mice. Follow-up preclinical studies using TNBC organoids and subsequent clinical trials will advance the efficacy and pharmacokinetic analysis of syntelin in treating

TNBC. In addition, modeling organoids from TNBC patients with a combination of the multi-target regime will enable us to consolidate the proteogenomic information for personalized precision therapy.

McKay Mullen[1,2,†], Fengrui Yang[1,2,†], Jun Cao[1,*], Yang Cao[3], Xu Liu[1,2], Gee Young Lee[2], Tao Li[1,4], William Yao[4], Zhihong Yang[1], Jiahai Zhang[1], Kela Johnson[2], Felix Aikhionbare[2], Yong Chen[3], Xinjiao Gao[1], Dongmei Wang[1], Xia Ding[4,*], Hadiyah-Nicole Green[2,5,*], Xing Liu ⓘD[1,2,*], and Xuebiao Yao[1,2]

[1]MOE Key Laboratory for Cellular Dynamics, Anhui Key Laboratory for Chemical Biology, CAS Center for Excellence in Molecular Cell Science, University of Science and Technology of China, Hefei 230027, China
[2]Keck Center for Oganoids Plasticity, Morehouse School of Medicine, Atlanta, GA 30310, USA
[3]Department of Hepatobiliary Surgery, Xijing Hospital, Xi'an 710032, China
[4]BUCM-USTC Collaborative Center for Parietal Cell Research, Beijing University of Chinese Medicine, Beijing 100029, China
[5]Ora Lee Smith Cancer Research Foundation, Atlanta, GA 30310, USA
[†]These authors contributed equally to this work.

*Correspondence to: Jun Cao, E-mail: caojun0811@ustc.edu.cn; Xia Ding, E-mail: dingx@bucm.edu.cn; Hadiyah-Nicole Green, E-mail: hgreen@msm.edu; Xing Liu, E-mail: xing1017@ustc.edu.cn

Edited by Haian Fu

References

Bianchini, G., Balko, J.M., Mayer, I.A., et al. (2016). Triple-negative breast cancer: challenges and opportunities of a heterogeneous disease. Nat. Rev. Clin. Oncol. *13*, 674–690.

Chen, J., Yao, Y., Gong, C., et al. (2011). CCL18 from tumor-associated macrophages promotes breast cancer metastasis via PITPNM3. Cancer Cell *19*, 541–555.

Ding, X., Yan, F., Yao, P., et al. (2010). Probing CENP-E function in chromosome dynamics using small molecule inhibitor syntelin. Cell Res. *20*, 1386–1389.

Huang, Y., Lin, L., Liu, X., et al. (2019). BubR1 phosphorylates CENP-E as a switch enabling the transition from lateral association to end-on capture of spindle microtubules. Cell Res. *29*, 562–578.

Kung, P.P., Martinez, R., Zhu, Z., et al. (2014). Chemogenetic evaluation of the mitotic kinesin CENP-E reveals a critical role in triple-negative breast cancer. Mol. Cancer Ther. *13*, 2104–2115.

Liu, X., Xu, L., Li, J., et al. (2020). Mitotic motor CENP-E cooperates with PRC1 in temporal control of central spindle assembly. J. Mol. Cell Biol. *12*, 654–665.

Rath, O., and Kozielski, F. (2012). Kinesins and cancer. Nat. Rev. Cancer *12*, 527–539.

Shen, Z. (2011). Genomic instability and cancer: an introduction. J. Mol. Cell Biol. *3*, 1–3.

Song, X., Liu, W., Yuan, X., et al. (2018). Acetylation of ACAP4 regulates CCL18-elicited breast cancer cell migration and invasion. J. Mol. Cell Biol. *10*, 559–572.

Yao, X., Anderson, K.L., and Cleveland, D.W. (1997). The microtubule-dependent motor centromere-associated protein E (CENP-E) is an integral component of kinetochore corona fibers that link centromeres to spindle microtubules. J. Cell Biol. *139*, 435–447.